GEOSCIENCE FRONTIERS 3(5) (2012) 647–660

available at www.sciencedirect.com

China University of Geosciences (Beijing)

GEOSCIENCE FRONTIERS

journal homepage: www.elsevier.com/locate/gsf

RESEARCH PAPER

Geochemistry of Late Triassic pelitic rocks in the NE part of Songpan-Ganzi Basin, western China: Implications for source weathering, provenance and tectonic setting

Yan Tang [a,*], Longkang Sang [b], Yanming Yuan [b], Yunpeng Zhang [c], Yunlong Yang [d]

[a] *College of Earth Science and Resources, Chang'an University, Xi'an 710054, PR China*
[b] *Faculty of Earth Sciences, China University of Geosciences, Wuhan 430074, PR China*
[c] *Xi'an Center of Geological Survey, China Geological Survey, Xi'an 710054, PR China*
[d] *SINOPEC Exploration Southern Company, Chengdu 610082, PR China*

Received 7 December 2011; accepted 5 January 2012
Available online 22 February 2012

KEYWORDS
Fine-grained sandstone-mudstone;
Geochemistry;
Source area weathering;
Provenance;
Tectonic setting;
Songpan-Ganzi Basin, China

Abstract Major, trace and rare earth element (REE) concentrations of Late Triassic sediments (fine-grained sandstones and mudstones) from Hongcan Well 1 in the NE part of the Songpan-Ganzi Basin, western China, are used to reveal weathering, provenance and tectonic setting of inferred source areas. The Chemical Index of Alteration (CIA) reflects a low to moderate degree of chemical weathering in a cool and somewhat dry climate, and an A-CN-K plot suggests an older upper continental crust provenance dominated by felsic to intermediate igneous rocks of average tonalite composition. Based on the various geochemical tectonic setting discrimination diagrams, the Late Triassic sediments are inferred to have been deposited in a back-arc basin situated between an active continental margin (the Kunlun-Qinling Fold Belt) and a continental island arc (the Yidun Island Arc). The Triassic sediments in the study area underwent a rapid erosion and burial in a proximal slope-basin environment by the petrographic data,

* Corresponding author.
E-mail addresses: tangyan2011@chd.edu.cn, breadwolf@163.com (Y. Tang).

Peer-review under responsibility of China University of Geosciences (Beijing).
doi:10.1016/j.gsf.2012.01.006

while the published flow directions of Triassic turbidites in the Aba-Zoige region was not supported Yidun volcanic arc source. Therefore, we suggest that the Kunlun-Qinling terrane is most likely to have supplied source materials to the northeast part of the Songpan-Ganzi Basin during the Late Triassic.

1. Introduction

The Songpan-Ganzi Basin of western China occupies a long narrow triangular area between the North China Block to the northeast, the Qiangtang Block to the southwest and the Yangtze Block to the southeast (Fig. 1), and is filled by a great thickness of Triassic flysch. The provenance of sediments and the tectonic nature of the Songpan-Ganzi Basin have attracted international attention for a long time (Gu, 1994; Nie et al., 1994; Bruguier et al., 1997; Gu et al., 2002; Su et al., 2005; Chen et al., 2006; Lan et al., 2006; Liu et al., 2006; She et al., 2006; Weislogel et al., 2006; Enkelmann et al., 2007; Roger et al., 2008, 2010; Weislogel, 2008), but the provenance and tectonic setting are still the subject of active debate.

Five possible provenances have been suggested on the basis of geochemical data: (1) the Dabie Orogenic Belt (Nie et al., 1994; Enkelmann et al., 2007); (2) the Kunlun-Qinling fold belt (Gu, 1994; Du et al., 1998; She et al., 2006; Enkelmann et al., 2007); (3) the North China Block (Weislogel et al., 2006; Enkelmann et al., 2007); (4) the Yangtze Block (Bruguier et al., 1997; Su et al., 2005; Chen et al., 2006; Lan et al., 2006; Weislogel et al., 2006); and (5) the Yidun Island Arc (Gu, 1994; Bruguier et al., 1997). There is a comparable variety of suggestions for the tectonic setting of sediments deposition, e.g., a continental island arc (Du et al., 1998; Su et al., 2005; Chen et al., 2006; Lan et al., 2006; Wang, 2007), a passive continental margin (Du et al., 1998; Wang, 2007), an active continental margin, and combinations of these. Several basin models have been proposed: (1) a back-arc basin (Klimetz, 1983; Şengör, 1984; Huang and Chen, 1987; Watson et al., 1987; Gu, 1994); (2) a foredeep/remnant-ocean basin (Nie et al., 1993, 1994; Zhou and Graham, 1996; Weislogel et al., 2006); and (3) an intracontinental rift basin (McElhinny et al., 1981; Chang, 2000; Meng and Zhang, 2000; Chen and Yang, 2003).

The study area is an important depocenter zone within the northeast of the Songpan-Ganzi flysch basin, marked by a rectangle in Fig. 1. In 2004, Sinopec Southern Exploration and Development Division drilled a 7000 m+ exploration well, the Hongcan Exploration Well 1 (indicated by a red star in Figs. 1 and 2), in Zoige County, Sichuan Province, to investigate oil and gas prospects. This well provides fresh core samples that supplement surface samples from previous oil and gas exploration studies. We present geochemical data for the Late Triassic pelitic rocks from the Hongcan Well 1 in an attempt to obtain new information about source area weathering, provenance and tectonic setting.

2. Geological setting

2.1. Review of tectonic framework

2.1.1. Songpan-Ganzi flysch

The Songpan-Ganzi flysch basin is a triangular structure situated at the junction of the North China Block, South China Block (including the Yangtze Block), and the North Tibet Block (Qiangtang Block)

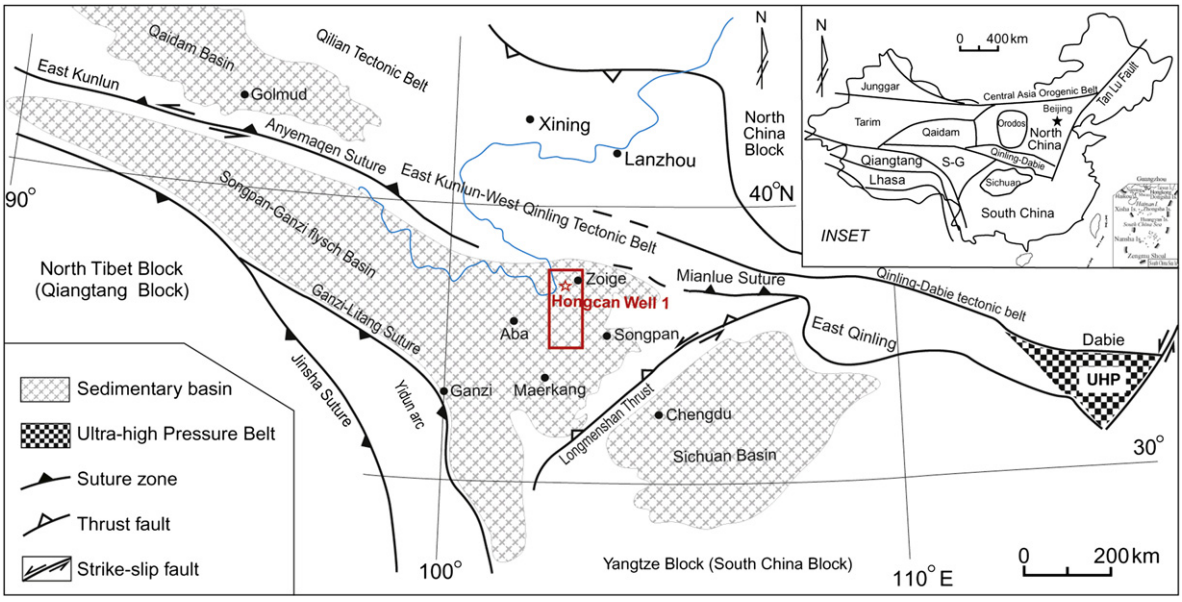

Figure 1 Simplified geological map of the Songpan-Ganzi Basin and district. Modified from the Sinopec South Exploration Company (2008) and Meng & Zhang (2000), showing the bounding Blocks and the major suture zones, as well as the distribution of the Dabie ultrahigh pressure. Rectangle indicates the study area, referring to Fig. 2 for enlargement; Hongcan Well 1 marked by red star. Inset: location of the Songpan-Ganzi complex relative to the major continental blocks and foldbelts after from Weislogel, 2008.

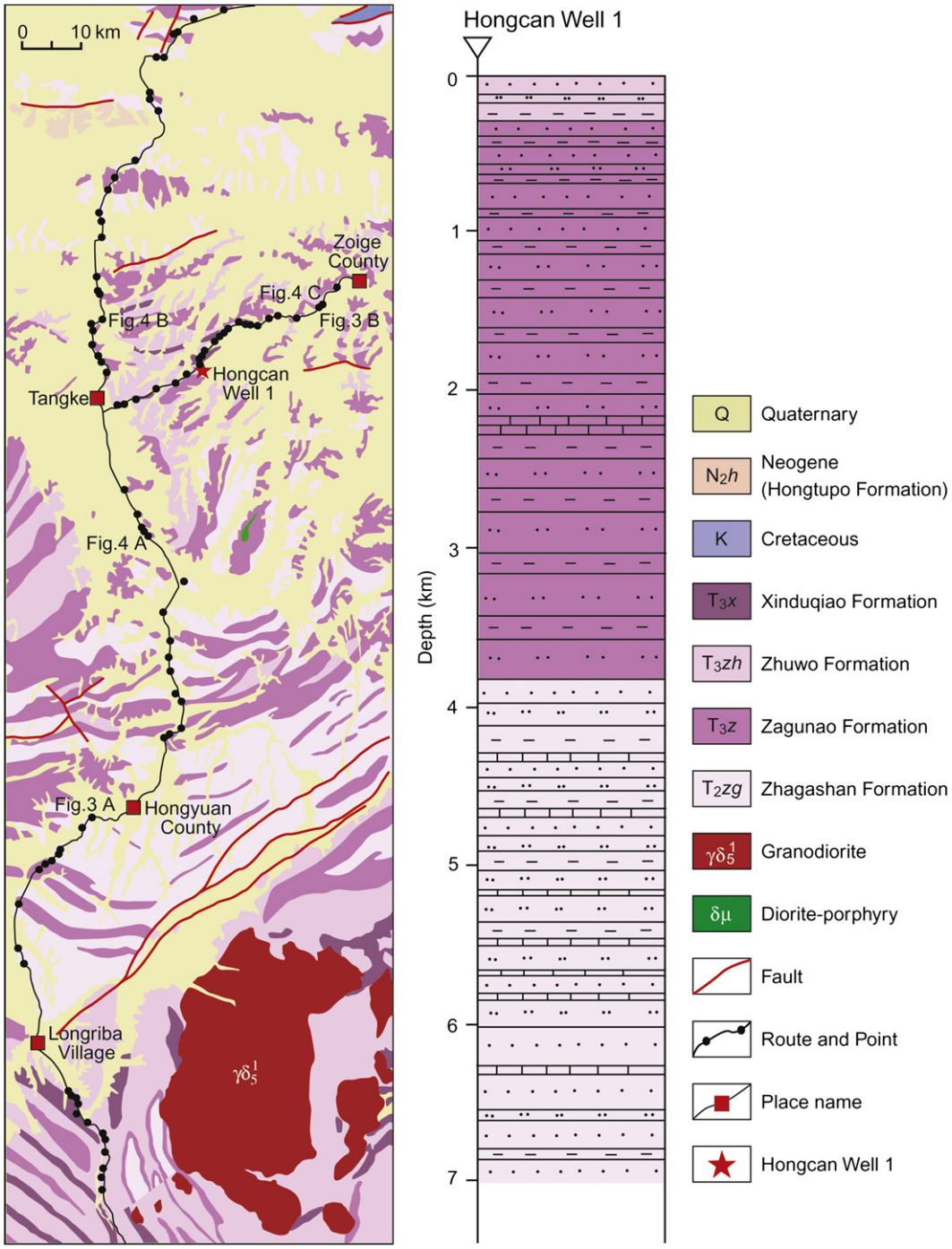

Figure 2 Geological map of the study area with simplified lithologic log of Hongcan Well 1 on the right. Modified from Sichuan Bureau of Geology and Mineral Resources (1984).

(Fig. 1). It is bounded to the north by the East Kunlun Orogenic Belt, to the northeast by the Qinling-Dabie or Central China Orogenic Belt, to the southeast by the Yangtze Block separated by the Longmenshan Thrust Belt, to the southwest by the Ganzi-Litang suture and Yidun Volcanic Arc. The Basin is mainly filled with continental slope-abyssal turbidites (Yang et al., 1996; Du et al., 1998; Yang and Xiong, 2000) with sparse fossils indicating a Middle–Upper Triassic age (Deng and Li, 1987; BGMRQP, 1991).

2.1.2. East Kunlun-West Qinling Belt

The West Qinling links laterally with the East Kunlun Belt to the west. The boundary between the East Kunlun-West Qinling Belt and the Songpan-Ganzi terrane is delineated by the A'nyemaqen-Mianlue suture. Plate convergence along the southern margin of the East Kunlun apparently ceased in late Middle Triassic or early Late Triassic time coeval with the main phase of Songpan-Ganzi flysch deposition (BGMRQP, 1991).

2.1.3. Qinling-Dabie Belt

The Qinling-Dabie Orogenic Belt has attracted international interest because of the UHP metamorphic rocks. It formed by the continent-continent collision between the South China Block and the North China Block during the Triassic. The Songpan-Ganzi Basin abuts the Qinling portion of the belt, while the Dabie Orogen continuing the Qinling Belt to the east mainly comprises a formation of Precambrian metamorphic rocks that includes coesite- and diamond-bearing eclogites and numerous Mesozoic granitoid plutons (Ma et al., 1998, 2000).

2.1.4. Yangtze Block

The Yangtze Block is separated from the Songpan-Ganzi basin along its eastern margin by the Longmenshan Thrust Belt. During the Late Palaeozoic–Early Mesozoic, successive carbonates with local interlayers of clastic rocks were deposited above the Yangtze Craton, overlain by a thick foreland sedimentary sequence of latest Triassic to Jurassic age (BGMRSP, 1991).

2.1.5. Yidun Volcanic Arc

The Yidun Volcanic Arc is separated from the southwest of the Songpan-Ganzi basin by Ganzi-Litang suture and from the eastern Qiangtang Block along the Jinshajiang suture. The Yidun Arc mainly consists of various mafic to felsic magmatic rocks.

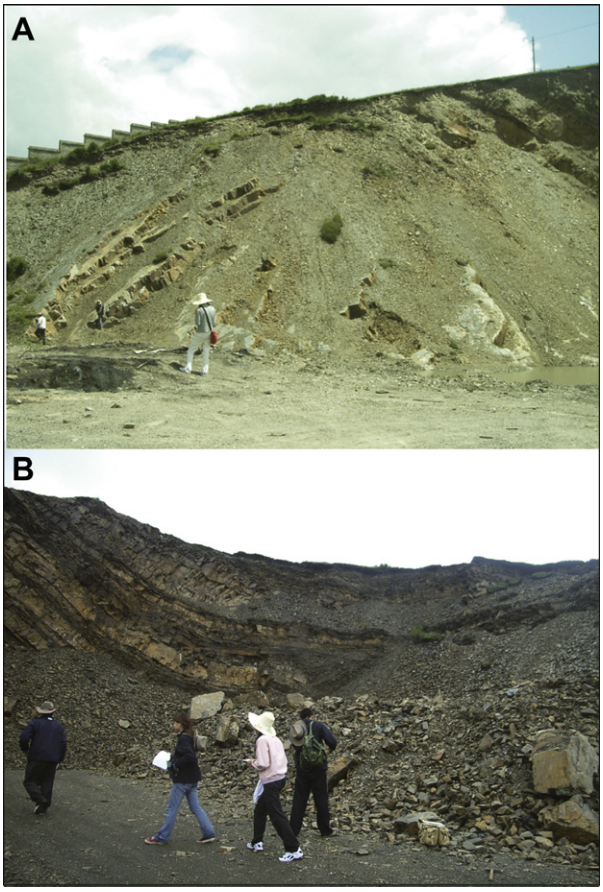

Figure 3 Outcrop of folds and associated Formations. Refer to Fig. 2 for locations. A: The hinge zone of anticline composed of Zhagashan Formation (T_2zg) in the core and Zagunao Formation (T_3z) in the two limbs. B: The syncline composed of Zhuwo Formation (T_3zh) in the core and Zagunao Formation (T_3z) in the two limbs.

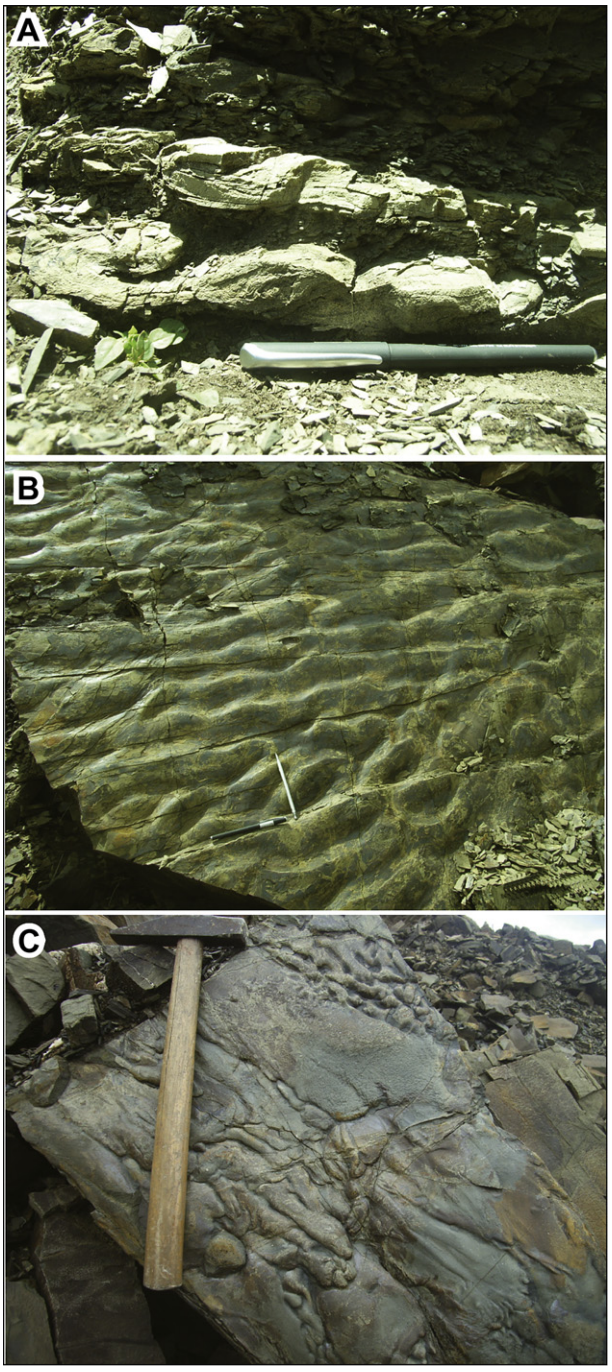

Figure 4 Outcrop of the sedimentary structures. Refer to Fig. 2 for locations. A is for convolute bedding developed in the Zagunao Formation (T_3z); B is for asymmetrical ripple and C is for flute cast observed in the Zhuwo Formation (T_3zh).

2.2. Stratigraphy

The Middle to Upper Triassic sedimentary sequence of the study area is locally covered by Quaternary sediments (Fig. 2). The Mesozoic basin sediments comprise the Xinduqiao (T_3x),

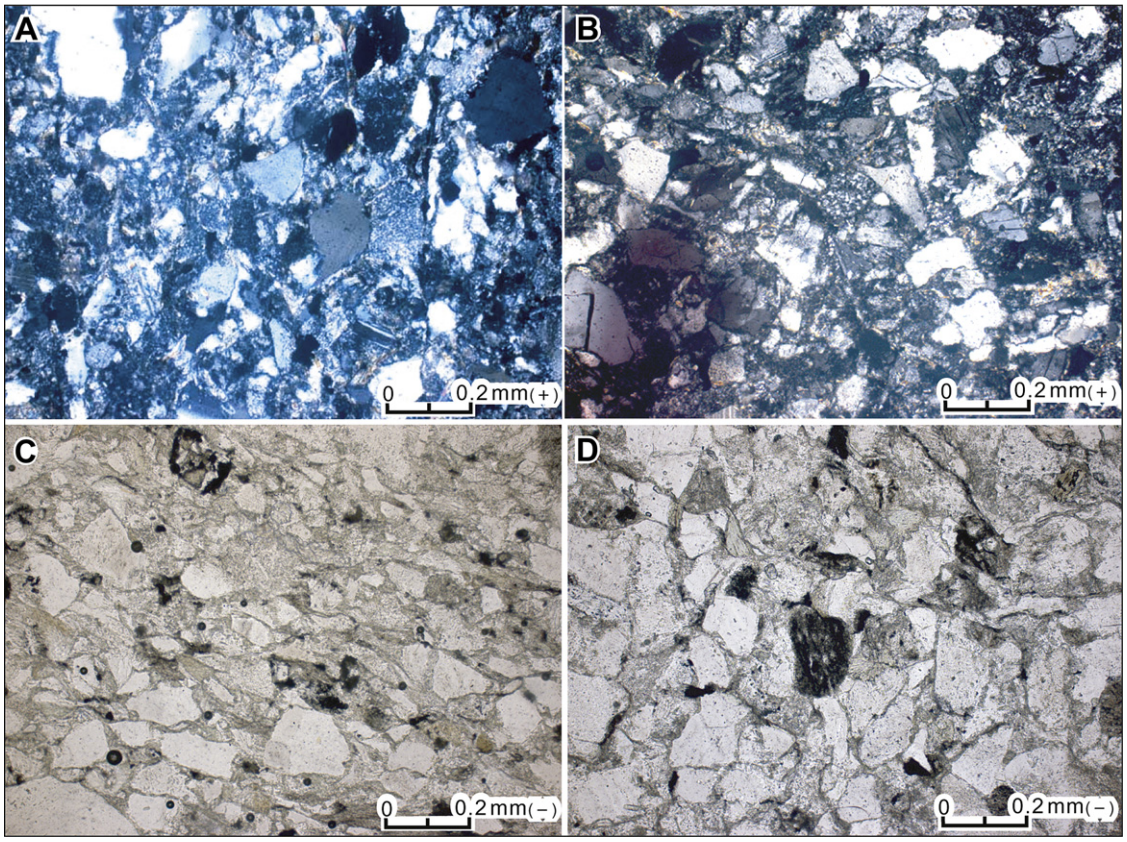

Figure 5 Photos of fine-grained sandstones in the thin-section from Hongcan Well 1. A is for fine-grained lithic feldspar sandstone from the depth of 526 m; B is from the depth of 1664 m; C is for fine-grained lithic feldspar sandstone from 2850 m; D is for fine-grained quartz feldspar sandstone from 3285 m.

Zhuwo (T_3zh), Zagunao (T_3z) and Zhagashan (T_2zg) formations of which the Hongcan Well 1 (Fig. 2) penetrates the Zhuwo (T_3zh) > 250 m, Zagunao (T_3z) 250 m to 3850 m and Zhagashan (T_2zg) > 3850 m (base not reached) formations SINOPEC Exploration Southern Company, 2008).

Brief descriptions of these formations from bottom to top are as follows:

Zhagashan Formation (T_2zg), with a thickness more than 1250 m, outcrops in Hongyuan County and the northern part of Zoige County. Zhagashan Formation strata commonly form the core of the anticline (Fig. 3A). It mainly consists of sandstones intercalated with occasional mudstones, and in the sandstones, the horizontal bedding and cross-bedding are developed, as well as the flute cast can be found. In Hongcan Well 1, this Formation can be divided into three sections: a lower section (T_2zg^1, 6015–7012.8 m) mainly consisting of sandstone accompanied by minor mudstone, limestone and siltstone; a middle section (T_2zg^2, 5065–6015 m) in which siltstone significantly increases, limestone is relatively abundant, and a significant reduction in the amounts of sandstone and mudstone; the upper section (T_2zg^3, 3825–5065 m) is mainly composed of sandstone, siltstone, mudstone and thinly bedded limestone.

Zagunao Formation (T_3z) (2000 m) has a conformable contact with the underlying Zhagashan Formation and outcrops in the southern and central parts of Zoige County and occasionally in the north. Zagunao Formation strata commonly form the limbs of the folds with a banded shape (Fig. 3). It is composed of sandstone

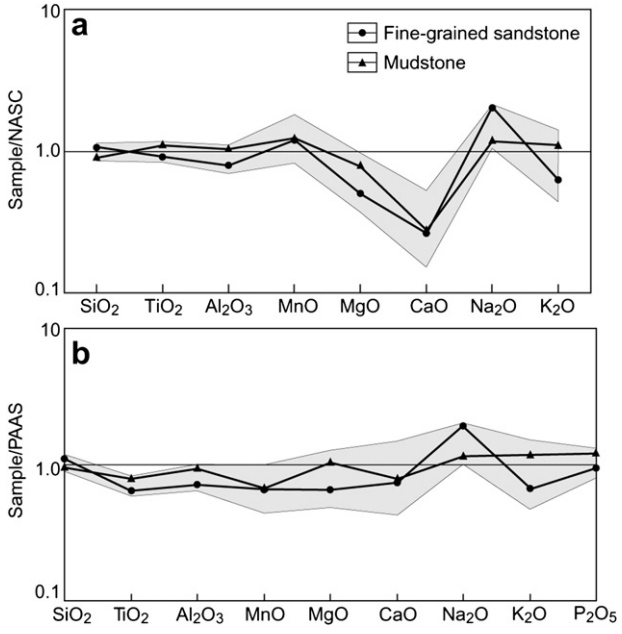

Figure 6 NASC- and PAAS-normalized major element diagrams for fine-grained sandstones and mudstone, Hongcan Well 1. PAAS data from Taylor and McLennan, 1985; NASC data from Gromet et al., 1984.

Table 1 Major element compositions (wt.%) for core samples from Hongcan Well 1.

SN	YS-1	YS-2	YS-3	YS-4	YS-5	YS-6	YS-7	YS-8	NASC	PAAS
Depth(m)	469	593	1316.6	1434.3	2223.2	2273.5	2647.8	2654.5		
Formation	T_3z	T_3z	T_3z	T_3z	T_3z	T_3z	T_3z	T_3z		
Litho	Fs	Md	Fs	Md	Md	Fs	Md	Fs		
SiO_2	73.51	62.65	70.37	59.60	59.85	65.39	57.44	69.76	64.80	62.40
TiO_2	0.63	0.76	0.60	0.80	0.83	0.77	0.77	0.59	0.70	0.99
Al_2O_3	12.12	15.13	12.48	18.70	19.17	16.18	18.57	13.51	16.90	18.80
Fe_2O_3	0.56	1.28	0.81	1.23	1.28	0.87	0.95	0.71		
FeO	2.75	4.75	4.78	5.95	5.15	4.10	5.05	4.05		
MnO	0.05	0.05	0.09	0.11	0.06	0.07	0.08	0.08	0.06	0.11
MgO	1.07	2.82	1.57	2.35	1.99	1.70	2.09	1.43	2.86	2.19
CaO	0.81	1.94	1.19	0.65	0.56	0.93	0.95	0.93	3.63	1.29
Na_2O	2.40	1.74	2.18	1.32	1.25	2.22	1.21	2.44	1.14	1.19
K_2O	2.39	3.11	1.76	4.06	4.65	3.16	5.63	2.66	3.97	3.68
P_2O_5	0.14	0.21	0.13	0.19	0.18	0.18	0.21	0.16		0.16
Fe_2O_3* + MgO	4.69	9.38	7.69	10.19	8.99	7.13	8.65	6.64		
Al_2O_3/TiO_2	19.24	19.91	20.80	23.38	23.10	21.01	24.12	22.90		
CIA	61.2	62.4	62.9	71.9	71.4	66.0	66.6	62.2		

Note: Major elements were analyzed using a 3080E1 X-ray Fluorescence (XRF) spectrometer at the Analytical Institute of the Bureau of Geology and Mineral Resources, Hubei Province. NASC—North American Shale Composite (Gromet et al., 1984); PAAS—Post-Archean Australian Shale (Taylor and McLennan, 1985); SN—sample number; Litho—lithology; Fs—fine-grained sandstone; Md—mudstone; depth is for Hongcan Well 1.

accompanied by mudstone, siltstone and minor slate, and the horizontal bedding, cross-bedding and the convolute bedding (Fig. 4A) develop in the sandstone, the flute cast can also be found. Two sections can be distinguished in Hongcan Well 1: an upper section (T_3z^2, 248–1291 m) mainly consisting of fine-grained sandstone and mudstone with minor siltstone and fine-grained sandstone interbedded with mudstone (less than half the thickness of the fine-grained sandstone); a lower section (T_3z^1, 1291–3825 m) consisting of mainly fine-grained sandstone with a small amount of mudstone and siltstone and including two thin layers of limestone.

Zhuwo Formation (T_3zh) (1700 m) is concordant with the underlying Zagunao Formation, outcrops widely throughout the study area, and Zhuwo Formation strata commonly form the trough of syncline (Fig. 3B). It is characterized by thin-, medium- to thick-bedded fine-grained sandstone regularly interbedded with mudstone. Sandstone increases and mudstone decreases from the bottom upwards. Here the sandstone develops grading bedding, as well as the asymmetrical ripple (Fig. 4B) and flute cast (Fig. 4C) can be seen locally. In Hongcan Well 1 (0–248 m), the Zhuwo Formation is mainly composed of sandstone, siltstone and mudstone, and the sandstone is regularly interbedded with mudstone with a small amount of siltstone. No limestone is present.

Xinduqiao Formation (T_3x) (2400 m) crops out in the southern and central parts of the Zoige Massif. It is mainly composed of dark-grey mudstone, slate and siliceous phyllite accompanied by brown-yellow thin-bedded fine-grained, feldspathic lithic sandstone. Slate

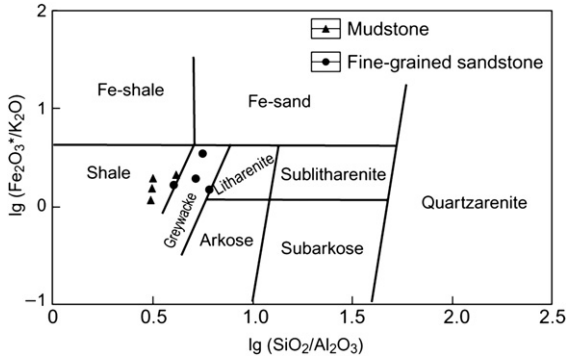

Figure 7 Lg (Fe_2O_3*/K_2O) versus lg (SiO_2/Al_2O_3) (after Herron, 1988) for the Late Triassic fine-grained sandstones and mudstones, Hongcan Well 1.

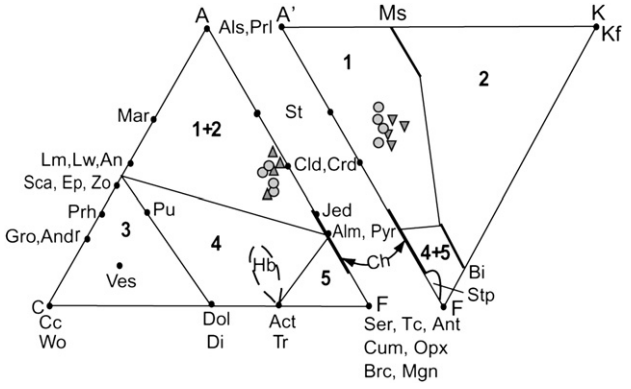

Figure 8 ACF-A'KF plots of Hongcan Well 1 fine-grained sandstones (filled circles) and mudstones (filled triangles) compared with chemical compositions of five very low-grade rock types and ideal mineral compositions (Lu and Sang, 2002). 1—pelitic rocks (Al_2O_3 excess); 2—felsic rocks (K_2O excess); 3—calcareous rocks; 4—basic igneous rocks; 5—magnesian rocks. Mineral abbreviations from Lu and Sang (2002).

Table 2 Trace element compositions (in ppm) for core samples from Hongcan Well 1.

SN	YS-1	YS-2	YS-3	YS-4	YS-5	YS-6	YS-7	YS-8	NASC	PAAS
Depth (m)	469	593	1316.6	1434.3	2223.2	2273.5	2647.8	2654.5		
Formation	T_3z	T_3z	T_3z	T_3z	T_3z	T_3z	T_3z	T_3z		
Litho	Fs	Md	Fs	Md	Md	Fs	Md	Fs		
Sc	6.8	12	7.8	15	16.7	11.8	17.1	8.8	15	16
Ni	17.4	31.1	25.6	41.2	43.9	32.4	53.4	25.2	58	55
Ga	12.7	20.9	13.7	24.5	27.3	21.2	26.7	17.3		
Nb	9.6	12.5	8.2	11.5	11.1	11.3	12.2	9.2	13	1.9
Ba	306	356	186	433	506	342	624	295	636	650
Ta	0.93	1.13	0.85	1.06	1.12	1.07	1.12	0.91	1.1	
Co	10.8	14.1	13.7	18.5	17.8	15.7	28.6	9.3	26	23
Cu	10	18.3	279	36.4	32.5	51.7	58.1	19.1		
Sr	133	143	131	94	98	120	97	114	142	200
V	71.8	92.3	71.6	142	149	104	139	68.5	130	96
Zn	63.1	95.3	86.1	124	134	97.2	127	130		
Th	8.8	10.4	7	9.3	9.6	8.2	11.1	6.7		
U	2.24	2.28	1.78	2	2.03	2.4	2.14	1.88		
Cr	53.9	67.5	52	65.7	66.7	58.1	68	47.9	125	110
Rb	92.5	131	72.7	175	190	129	215	104	125	160
Zr	245	182	183	184	189	204	187	174	200	210
Hf	6.9	5	4.8	4.9	5.1	5.5	4.9	4.9	6.3	5
Cr/Zr	0.22	0.37	0.28	0.36	0.35	0.28	0.36	0.28	0.63	0.52
Th/Sc	1.29	0.87	0.9	0.62	0.57	0.69	0.65	0.76		

Note: Trace elements were analyzed utilizing an inductively coupled plasma atomic emission spectrometer (ICP-AES) at the Analytical Institute of the Bureau of Geology and Mineral Resources, Hubei Province. Other legends referred to Table 1.

and siliceous phyllite occurs in the Longriba area in a contact aureole of an intrusion, and dark-grey lenses of crystalline limestone are developed in mudstone in the Zoige area. The formation is in conformable contact with the underlying Zhuwo Formation.

Combined the field observation and thin-section analysis, the Triassic sediments in the study area mainly consist of sandstone and mudstone, and the sandstone (Fig. 5) is characterized by poor roundness and sorting, grain supported, with low compositional and textural maturity; also the sedimentary structures such as grading bedding, convolute bedding and flute mould can be observed, all of these reflect a turbidity current depositional origin in a proximal slope-basin environment with rapid erosion and burial (Tang, 2011; see Figs. 3–6). Moreover, samples from Hongcan Well 1 have undergone high temperature diagenesis, very low to low-grade metamorphism. Above 2800 m, the metamorphic grade is that of the high grade diagenetic zone. Below 2800 m the metamorphic grade is anchizone with only a few samples attaining epizone conditions at the base (6000–7000 m) (Tang et al., 2007).

3. Samples and analytical methods

Eight representative core samples of mudstone and fine-grained sandstone from Hongcan Well 1 were analyzed for major elements, trace elements and REE's at the Analytical Institute of the Bureau of Geology and Mineral Resources, Hubei Province. Major elements were analyzed using a 3080E1 X-ray Fluorescence (XRF) spectrometer with an accuracy <1%. Trace and rare earth element analyses were made using an inductively coupled plasma atomic emission spectrometer (ICP-AES), with an analytical precision <5%.

4. Results

4.1. Major elements

Major element compositions of the eight representative core samples are listed in Table 1. Average compositions of North American Shale Composite (NASC; Gromet et al., 1984) and Post-Archean Australian Shale (PAAS; Taylor and McLennan, 1985) are also listed for comparison.

Fig. 6a, b show variations of major elements (grey fields) normalized to NASC (a) and PAAS (b) and indicate that compositions are essentially comparable with those of NASC and PAAS, except for CaO which is significantly lower than NASC, and Na_2O which is generally higher than NASC and PAAS. Fig. 6a, b also differentiate the Hongcan Well 1 mudstones and fine-grained sandstones with fine-grained sandstones having higher SiO_2, Na_2O, and lower Al_2O_3, K_2O than mudstones reflecting higher modal quartz and acid plagioclase in the former, and a higher proportion of clay minerals in the latter.

Fig. 7 shows a lg-lg plot of (SiO_2/Al_2O_3) vs. (Fe_2O_3/K_2O) after Herron (1988), where mudstones plot within the shale field and fine-grained sandstones cluster in the greywacke field. A combined ACF and A'KF diagram (Fig. 8) shows mudstones (or shale) and fine-grained sandstones (or greywacke) plot within the field of Al-rich pelitic sediments.

4.2. Trace elements

Table 2 demonstrates the concentrations of trace elements from the Hongcan Well 1 sediments. Fig. 9a, b show ranges of composition of

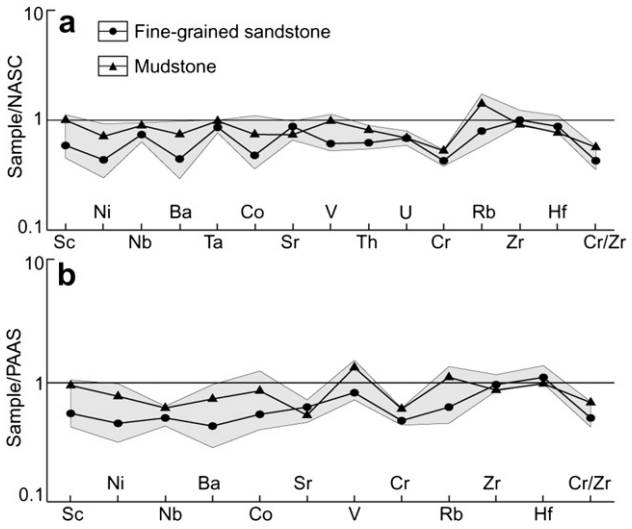

Figure 9 NASC- and PAAS-normalized trace element compositions of fine-grained sandstones and mudstones, Hongcan Well 1. PAAS data from Taylor and McLennan, 1985; NASC data from Gromet et al., 1984.

trace elements (grey fields) normalized to NASC (a) and PAAS (b), and indicate that abundances are lower than NASC and PAAS, notably Cr/Zr ratios. Most trace elements are concentrated in mudstone compared to fine-grained sandstones, except for Sr, Zr and Hf. Values of Cr/Zr may be used to indicate the relative contributions of mafic and felsic source rocks to the sediments (Wronkiewicz and Condie, 1989). Cr/Zr values in all studied samples are lower than 1 (0.22–0.37) (Table 2), indicating a felsic source.

4.3. Rare earth elements

Rare earth element concentrations of core samples are listed in Table 3 and Fig. 10 shows that they have similar chondrite-normalized REE patterns to NASC and PAAS, characterized by LREE enrichment and negative Eu anomalies, indicating that the main sedimentary source were continental crustal rocks. REE patterns display a significant HREE depletion, $(La/Yb)_n$ 6.69 to 10.04 average 7.93 (Table 3). LREE's are more strongly fractionated than HREE's because LREE patterns are steep while HREE patterns are flat. All the samples display clear negative Eu anomalies [δEu = 0.65–0.73 average 0.69, very close to that of NASC (δEu = 0.69) and PAAS (δEu = 0.64) (Table 3)]. They also have slightly negative Ce anomalies (δCe = 0.77–0.89; av. = 0.84, less than NASC and PAAS), indicating that the degree of oxidation of the rocks in the source area was lower than that of NASC, possibly because the area escaped strong chemical weathering in a cold climate.

5. Discussion

5.1. Geochemistry and weathering

The chemical index of alteration (CIA) is useful for estimating the degree of chemical weathering in sedimentary rocks. It was defined by Nesbitt and Young (1982) as CIA = $[Al_2O_3/(Al_2O_3 + CaO^* + Na_2O + K_2O)] \times 100$, where CaO* represents Ca in silicate minerals only (i.e., excluding calcite, dolomite and apatite) (Fedo et al., 1995). An approximate correction for carbonate content can be made by assuming reasonable Ca/Na ratios in silicate materials (McLennan et al., 1993). After

Table 3 Rare earth element concentrations (in ppm) for core samples from Hongcan Well 1.

SN	YS-1	YS-2	YS-3	YS-4	YS-5	YS-6	YS-7	YS-8	NASC	PAAS
Depth (m)	469	593	1316.6	1434.3	2223.2	2273.5	2647.8	2654.5		
Formation	T_3z	T_3z	T_3z	T_3z	T_3z	T_3z	T_3z	T_3z		
Litho	Fs	Md	Fs	Md	Md	Fs	Md	Fs		
La	34.01	43.12	26.71	35.85	37.3	33.82	39.07	27.11	32	38
Ce	57.86	80.81	49.99	73.49	75.8	65.92	75.71	52.75	73	80
Pr	7.99	9.69	6.8	9.14	9.39	8.98	10.21	7	7.9	8.83
Nd	28.54	36.77	24.8	34.66	34.31	32.02	36.94	25.02	33	33.9
Sm	5.18	6.55	4.9	6.99	6.41	6.21	7.35	5.11	5.7	5.55
Eu	1.16	1.33	1.06	1.52	1.36	1.37	1.56	1.1	1.24	1.08
Gd	4.45	5.75	4.59	6.48	5.46	5.45	6.52	4.34	5.2	4.66
Tb	0.7	0.88	0.78	1.08	0.91	0.93	1.08	0.68	0.85	0.77
Dy	4.12	5.02	4.39	6.18	5.46	5.39	6.29	3.99	6.2	4.68
Ho	0.85	1.02	0.87	1.26	1.1	1.1	1.31	0.83	1.04	0.99
Er	2.41	2.86	2.52	3.47	3.06	3.12	3.72	2.34	3.4	2.85
Tm	0.37	0.46	0.4	0.56	0.47	0.51	0.58	0.36	0.5	0.4
Yb	2.39	2.78	2.44	3.47	2.82	3.1	3.66	2.21	3.1	2.82
Lu	0.37	0.42	0.38	0.53	0.41	0.47	0.56	0.34	0.48	0.43
Y	21.12	25.47	23.97	30.47	26.53	26.84	33.38	20.23	27	
δCe	0.77	0.86	0.82	0.89	0.89	0.83	0.83	0.84	1.01	0.95
δEu	0.73	0.65	0.68	0.69	0.69	0.71	0.68	0.7	0.69	0.64
(La/Yb)n	9.21	10.04	7.08	6.69	8.56	7.06	6.91	7.94	6.68	8.72

Note: REEs were analyzed by an inductively coupled plasma atomic emission spectrometer (ICP-AES) at the Analytical Institute of the Bureau of Geology and Mineral Resources, Hubei Province. Other legends referred to Table 1.

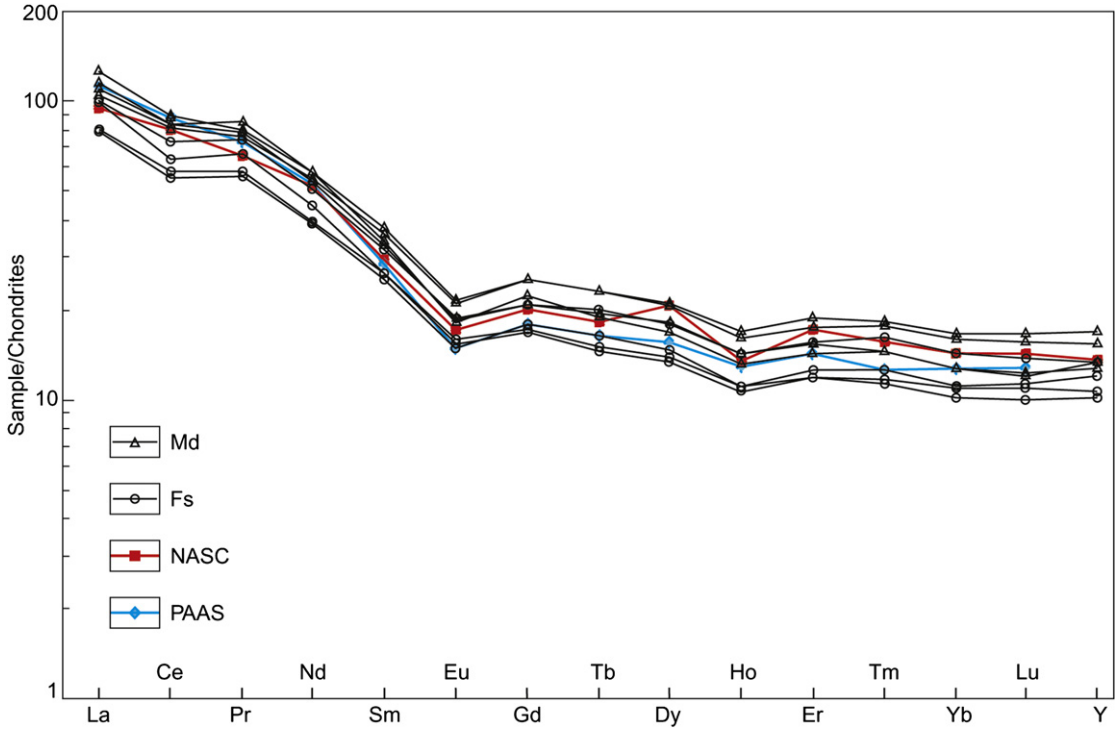

Figure 10 Chondrite normalized REE patterns for fine-grained sandstone (Fs) and mudstone (Md), Hongcan Well 1, compared with PAAS and NASC patterns (PAAS data from Taylor and McLennan, 1985; NASC data from Gromet et al., 1984).

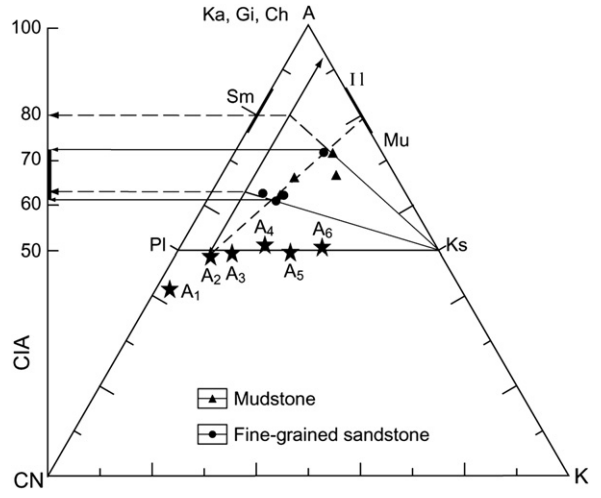

Figure 11 A-CN-K ternary diagram of molecular proportions of Al_2O_3-(CaO^*+Na_2O)-K_2O for fine-grained sandstones and mudstones from Hongcan Well 1 (Nesbitt & Young, 1984). The CIA scale shown at the left side of the figure for comparison. Ideal compositions of minerals labelled: Pl, plagioclase; Ks, K-feldspars; Il, illite; Mu, muscovite; Sm, smectite; Ka, kaolinite; Gi, gibbsite; Ch, chlorite. Stars: average compositions of gabbro (A_1), tonalite (A_2), granodiorite (A_3), granite (A_4), A-type granite (A_5) and charnockite (A_6) from Fedo et al. (1997). Solid arrow indicates the predicted weathering trend for tonalite; dotted arrow shows the actual weathering trend for the samples.

correcting for Ca in phosphate using P_2O_5 (i.e. $CaO^* = [CaO] - 10/3[P_2O_5]$), provided that the remaining mole fraction of $CaO \leq Na_2O$, acceptable CaO^* values are obtained when $CaO > Na_2O$ and CaO^* is assumed to be equivalent to Na_2O. CIA values between 50 and 60 indicate a low degree of chemical weathering, between 60 and 80 moderate chemical

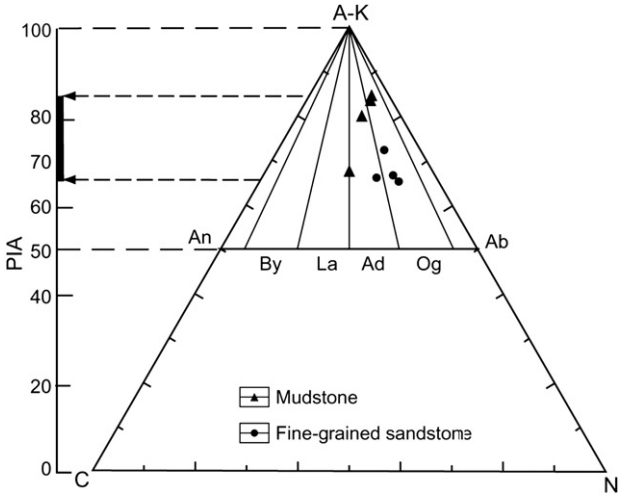

Figure 12 Fine-grained sandstones and mudstones from Hongcan Well 1 plotted in terms of (A-K)-C-N ternary diagram where (A-K) = (Al_2O_3-K_2O), C = CaO^* and N=Na_2O. Scale at left indicates plagioclase index of alteration from Fedo et al. (1995). An: anorthite; By: bytownite; La: labradorite; Ad: andesine; Og: oligoclase; Ab: albite.

weathering, with values >80 indicating extreme chemical weathering (Fedo et al., 1995). The CIA is also a useful tool for providing a semi-quantitative assessment of paleoclimate in the source area because a large amount of aluminous clay minerals generally forms by intensive chemical weathering under tropical conditions and gives CIA values of 80–100. In contrast, under glacial environments where abrasion is dominant over chemical weathering, common CIA values range from 50 to 70 (Nesbitt and Young, 1982). Calculated CIA values of the studied samples range between 61.2 and 71.9 (average 65.6; Table 1 and Fig. 11) indicating that the source area may have been subject to a moderate degree of weathering in a cool climate without abundant rainfall.

Molar proportions of Al_2O_3 (A), $CaO^* + Na_2O$ (CN) and K_2O (K) in the Late Triassic Hongcan Well 1 samples are plotted in A-CN-K compositional space (Fig. 11) after Nesbitt and Young (1984, 1989) to estimate trends of chemical weathering, metasomatism and source rock compositions. Weathering trends might be predicted to be parallel to the A-CN join during the initial stages because Na and Ca are removed by chemical weathering of plagioclase feldspars as shown by solid arrow in Fig. 11. As weathering continues, K-feldspars should also have been weathered releasing K and shifting the residual composition towards the Al_2O_3 apex. However, the actual trend of the Hongcan well 1 samples (dotted line) is subparallel to the A-CN join towards the compositions of illite and muscovite, different from the predicted weathering trend (solid arrow). This divergent trend was possibly caused by potassium metasomatism (c.f. Fedo et al., 1996, 1997) or K_2O enrichment during the sedimentary process, and the mudstones were more profoundly affected than fine-grained sandstones (Fig. 11). The effect of metasomatism can be corrected for by projection of lines from the K-apex through the data points to the ideal weathering line (solid arrow). Such a technique should give an approximation of the original CIA values (Fedo et al., 1995). Corrected CIA values range from 63 to 80 in Fig. 8 (on the left scale of CIA marked by two parallel dotted arrows), still displaying moderate chemical weathering. An additional advantage of the A-CN-K ternary plot is that it enables estimation of source rock compositions by backward projection of the weathered samples to a point on the feldspar line. The intersection point provides an approximate ratio of plagioclase to

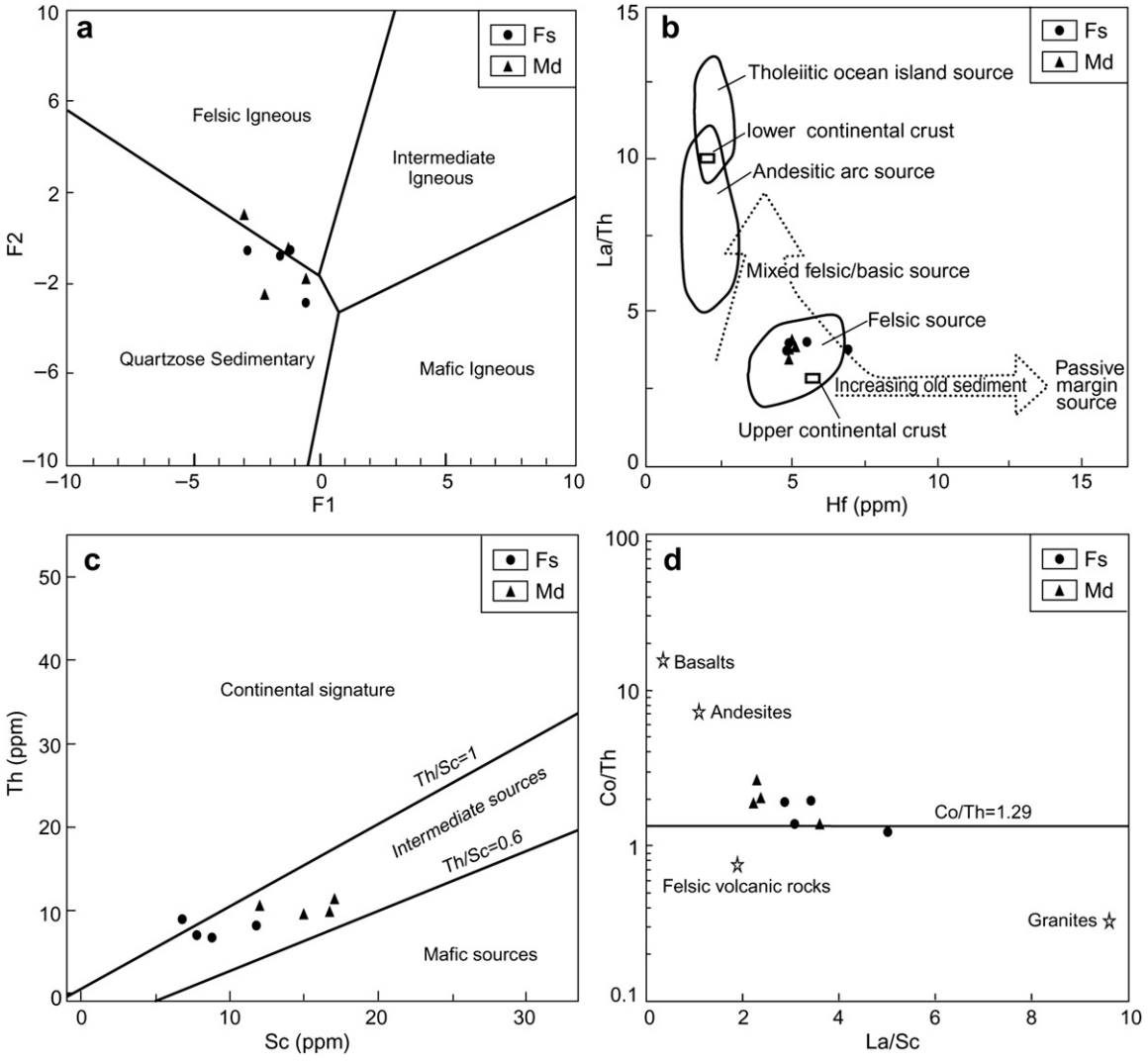

Figure 13 Discrimination diagrams for provenance of Hongcan Well 1 Late Triassic fine-grained sandstones (Fs) and mudstones (Md). a: Discriminant function diagram (Roser and Korsch, 1988); b: La/Th-Hf diagram (Floyd and Leveridge, 1987); c: Th versus Sc diagram from McLennan et al. (1993); d: Co/Th-La/Sc diagram (after Gu et al., 2002).

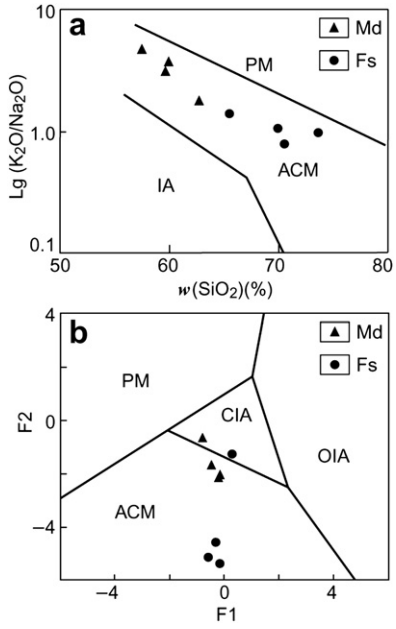

Figure 14 Major element tectonic setting discrimination diagrams for fine-grained sandstones (Fs) and mudstones (Md), Hongcan Well 1. a: $Lg(K_2O/Na_2O)$ vs. SiO_2 (Roser and Korsch, 1986); b: Discriminant function diagram (Bhatia, 1983). IA, island arc; ACM, active continental margin; PM, passive margin; CIA, continental island arc; OIA, oceanic island arc.

K-feldspar in the source rock. Fig. 11 shows that the weathering trend suggests a tonalitic provenance.

Molar proportions of Al_2O_3 (minus Al associated with K), CaO* and Na_2O are plotted in the (A-K)-C-N diagram of Fedo et al. (1997) in order to understand and monitor the evolution of plagioclase weathering in the Late Triassic sediments (Fig. 12). The vertical dimension on the (A-K)-C-N triangle corresponds to the plagioclase index of alteration (PIA = $[(Al_2O_3-K_2O)/(Al_2O_3 + CaO^* + Na_2O-K_2O)] \times 100$) of Fedo et al. (1995). PIA values of around 50 for fresh rocks and values approaching 100 indicate significant production of secondary aluminous clay minerals (Fedo et al., 1997). Fig. 12 shows that the samples are weathering products of parent material enriched in plagioclase feldspars in the range An_{10} to An_{50} (oligoclase [Og] to andesine [Ad]) with PIA values between 63 and 82. Fine-grained sandstones have lower PIA values than mudstone, suggesting that secondary aluminous clay minerals are concentrated in mudstone.

To summarize, we conclude that the Late Triassic pelitic sediments in the study area could have been derived by weathering of a tonalite-dominated source terrane that underwent low to moderate chemical weathering in a cool and relatively dry climate.

5.2. Geochemistry and provenance

Roser and Korsch (1988) proposed a provenance discriminant diagram based on major elements to distinguish mafic, intermediate, felsic igneous rocks from quartzose sedimentary rocks.

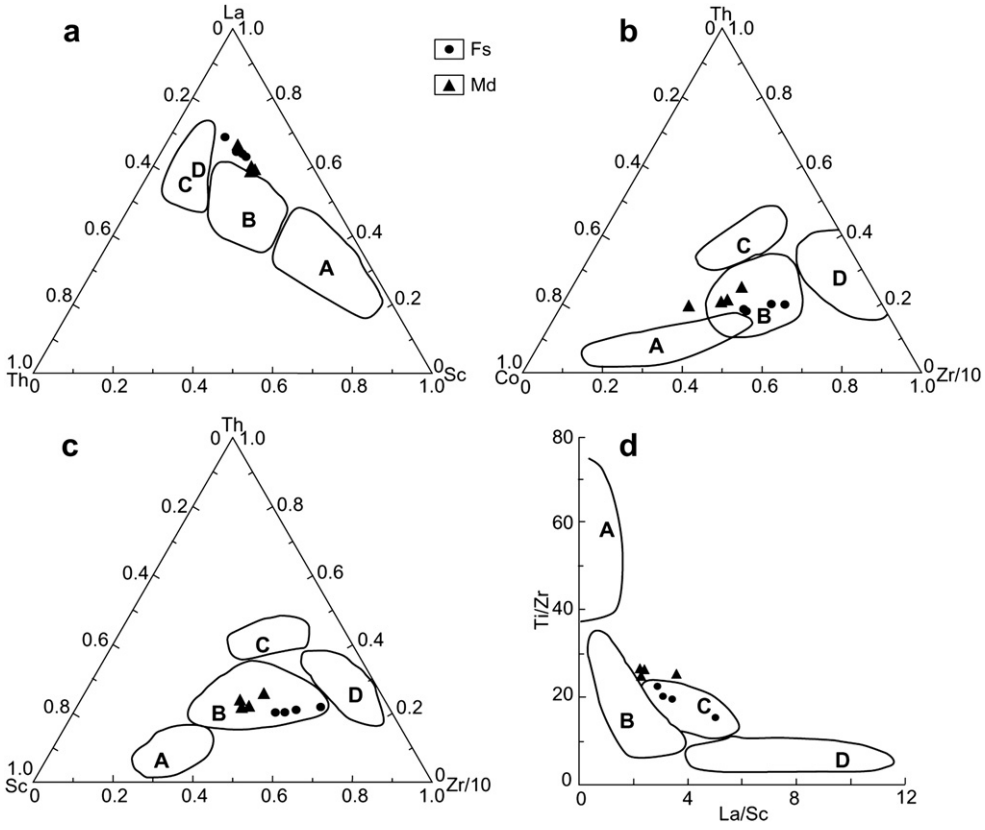

Figure 15 Trace element tectonic setting discrimination diagrams (Bhatia and Crook, 1986) for fine-grained sandstones (Fs) and mudstones (Md), Hongcan Well 1. a: La-Th-Sc; b: Th-Co-Zr/10; c: Th-Sc-Zr/10; d: Ti/Zr vs. La/Sc. A—oceanic island arc; B—continental island arc; C—active continental margin; D—passive margin.

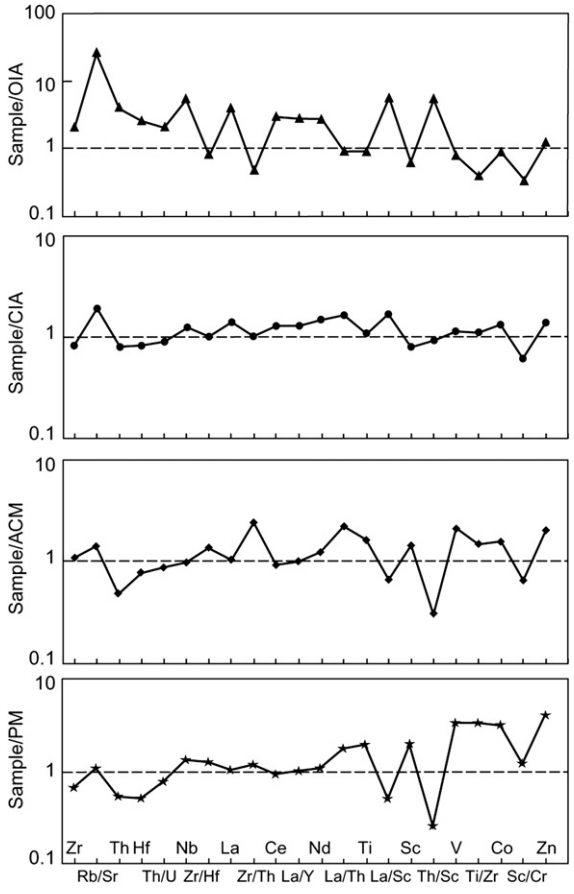

Figure 16 Normalized multi-element and element ratio diagrams for fine-grained sandstones (filled circles) and mudstones (filled triangles), Hongcan Well 1. OIA = oceanic island arc; CIA = continental island arc; ACM = active continental margin; PM = passive margin. Normalized values from Bhatia and Crook (1986).

Most of the Hongcan Well 1 samples cluster near to a line between felsic igneous and quartzose sedimentary fields (Fig. 13a).

Hayashi et al. (1997) pointed out that the ratio of Al_2O_3/TiO_2 in shales should be similar to that of their parent rocks and therefore the Al_2O_3/TiO_2 ratio can be used as a significant indicator of source rocks. Ratios exhibiting higher values (>21) indicate that sediments were derived from felsic source rocks (Hayashi et al., 1997). The average value of Al_2O_3/TiO_2 in the studied pelitic rocks is 21 (range of 19.2 to 24.1 in Table 1), reflecting a felsic to intermediate source. A plot of La/Th against Hf proposed by Floyd and Leveridge (1987) shows that almost all the Hongcan Well 1 samples fall into the field of felsic sources (Fig. 13b). A Th versus Sc plot (Fig. 13c), after McLennan et al. (1993), reveals a continental source to an intermediate component. Similarly, in a Co/Th-La/Sc diagram (Fig. 13d) from Gu et al. (2002), most samples plot near to or above a horizontal line at Co/Th = 1.29, indicating a felsic to intermediate igneous source. Finally, the REE patterns in Fig. 10 are characterized by enrichment of LREE, negative Eu anomalies and relatively flat HREE patterns, suggesting a felsic protolith.

Therefore, the main source of the Hongcan well 1 sediments was old upper continental crust dominated by felsic to intermediate igneous rocks of average composition of tonalite with no mafic or mature polycyclic quartzose detritus.

5.3. Geochemistry and tectonic setting

Geochemical data can also be used to decipher the ancient tectonic settings of sedimentary rocks (Maynard et al., 1982; Bhatia, 1983; Roser and Korsch, 1985, 1986, 1988; Bhatia and Crook, 1986). In Fig. 14a of Roser and Korsch (1986), the studied samples plot exclusively in the active continental margin (ACM) field. Plotting chemical analyses on the discrimination diagram of Bhatia (1983) shows that the Triassic sediments might have been deposited in either an active continental margin or a continental island arc setting (Fig. 14b).

Bhatia and Crook (1986) suggested several discrimination diagrams based on trace elements including REE's. Almost all our samples plot in the continental island arc fields of their ternary La-Th-Sc diagram (Fig. 15a), Th-Co-Zr/10 diagram (Fig. 15b) and Th-Sc-Zr/10 diagram (Fig. 15c) except for some samples in Fig. 15a that plot nearby. Most of Hongcan Well 1 samples plot in the active continental margin field of the bivariate Ti/Zr vs. La/Sc diagram (Fig. 15d). When normalized to standard tectonic settings (Fig. 16), the Hongcan Well 1 Late Triassic sediments reflect deposition in a continental island arc setting. Table 4 shows that our samples have REE values and ratios between those of continental island arc and active continental margin sediments.

Combining indications from all discrimination diagrams, we conclude that Late Triassic deposition in the study area probably took place in a transitional tectonic setting from an active continental margin to a continental island arc. If this is correct, the Triassic sediments were probably deposited in a back-arc basin situated between an active continental margin (the Kunlun-Qinling Fold Belt) and a continental island arc (the Yidun Volcanic Arc) (Fig. 17), although a Yidun Volcanic Arc source is not supported by flow directions of Triassic turbidites in the Aba-Zoige region (Du et al., 1998). Petrographical data reflected a proximal slope-basin environment with rapid erosion and burial. We therefore suggest that the Kunlun-Qinling terrane is most likely to have supplied source materials to the northeast part of the Songpan-Ganzi Basin during the Late Triassic.

Table 4 Discriminating REEs and ratios for Triassic samples (after Bhatia, 1983).

Tectonic settings	La	Ce	∑REE	La/Yb	(La/Yb)n	Eu/Eu*
Oceanic island arc	8 ± 1.7	19 ± 3.7	58	4.2 ± 1.3	2.8 ± 0.9	1.04 ± 0.11
Continental island arc	27 ± 4.5	59 ± 8.2	146	11 ± 3.6	7.5 ± 2.5	0.79 ± 0.13
Active continental margin	37	78	186	12.5	8.5	0.6
Passive margin	39	85	201	15.9	10.8	0.56
Triassic samples[a]	34.62	66.54	193.95	12.26	7.93	0.69

[a] Values are obtained from the average values of studied samples in Hongcan Well 1. Eu/Eu* = δEu, Eu* = (Sm + Gd)/2.

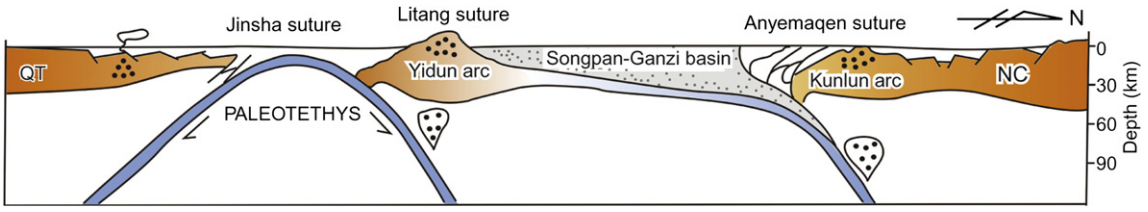

Figure 17 A sketch cross-section of back-arc basin between the Kunlun arc and the outboard Yidun arc modified from Weislogel (2008) and Roger et al. (2010). QT = Qiangtang Block; NC = North China Block.

6. Conclusions

Geochemical data of Late Triassic fine-grained sandstones and mudstone from Hongcan Well 1 in the northeastern part of the Songpan-Ganzi Basin indicates their source area weathering, provenance and the tectonic setting in which they were deposited. Combined ACF-A'KF diagrams indicate that all samples (mudstone and fine-grained sandstones) are Al-rich pelitic rocks. Most of their major elements are comparable with NASC and PAAS, except that CaO is significantly lower than NASC and Na_2O is generally higher than NASC and PAAS. Mudstones show higher contents of Al_2O_3, K_2O and ferromagnesian trace elements (such as Co, Cr, Ni, Sc, etc), and lower concentrations of SiO_2, Na_2O, Sr, Zr and Hf than associated fine-grained sandstones. Uniform REE patterns resemble upper continental crust, displaying LREE enrichment, flat HREE profiles, and significant negative Eu-anomalies. Chemical Index of Alteration (CIA) values indicate that the source area underwent moderate chemical weathering in a cold climate, and an A-CN-K ternary diagram suggests a dominant tonalitic source. Plagioclase Index of Alteration (PIA) values reflect a moderate degree of plagioclase weathering and an (A-K)-C-N triangle shows that the plagioclase of the source rocks was predominantly oligoclase and andesine. Various other provenance discrimination diagrams show that the source area was dominated by felsic to intermediate igneous rocks of generally tonalitic composition. Major and trace element compositions suggest two possible tectonic settings: an active continental margin and a continental island arc. If this is correct, the Triassic sediments were probably deposited in a back-arc basin situated between an active continental margin (the Kunlun-Qinling Fold Belt) and a continental island arc (the Yidun Volcanic Arc). Combining published data and our petrogrphical data, we conclude that the Kunlun-Qinling terrane is most likely to have supplied source materials to the northeast part of the Songpan-Ganzi Basin during the Late Triassic.

Acknowledgments

The research was supported by the SINOPEC Exploration Southern Company (the National Oil and Gas Special Projects XQ-04) and the Special Fund for Basic Scientific Research of Central Colleges, Chang'an University (CHD2011JC185). After editorial acceptance, Roger Mason corrected the English of a draft of this manuscript but he is not responsible for scientific conclusions.

References

BGMRQP (Bureau of Geology and Mineral Resources of Qinghai Province), 1991. Regional Geology of Qinghai Province. Geological Publishing House, Beijing, 138–177 (in Chinese).

BGMRSP (Bureau of Geology and Mineral Resources of Sichuan Province), 1991. Regional Geology of Sichuan Province. Geological Publishing House, Beijing, 218–230 (in Chinese).

Bhatia, M.R., 1983. Plate tectonics and geochemical composition of sandstone. The Journal of Geology 91, 611–627.

Bhatia, M.R., Crook, K.A.W., 1986. Trace element characteristics of graywackes and tectonic setting discrimination of sedimentary basins. Contributions to Mineralogy and Petrology 92, 191–193.

Bruguier, O., Lancelot, J.R., Malavieille, J., 1997. U-Pb dating on single detrital zircon grains from the Triassic Songpan-Ganzi flysch(central China): provenance and tectonic correlations. Earth and Planetary Science Letters 152, 217–231.

Chang, E.Z., 2000. Geology and tectonics of the Songpan-Ganzi fold belt, southwestern China. International Geology Review 42, 813–831.

Chen, Y.L., Tang, J.R., Liu, F., et al., 2006. Elemental and Sm-Nd isotopic geochemistry of clastic sedimentary rocks in the Garzê-Songpan block and Longmen Mountains. Geology in China 33 (1), 109–118 (in Chinese with English abstract).

Chen, M., Yang, H., 2003. Triassic sedimentary basins and paleontological features on the Qinghai-Xizang Plateau. Sedimentary Geology and Tethyan Geology 23 (2), 14–19 (in Chinese with English abstract).

Deng, K.L., Li, G.J., 1987. Studies on the turbidites of the Xikang Group in the Northwestern Sichuan. In: Collected Works on Lithofacies and Paleography. Geological Publishing House, Beijing, pp. 219–238 (in Chinese).

Du, D.X., Luo, J.N., Hui, L., 1998. Sedimentary facies and palaeogeography of the Triassic sedimentary basins in the Baryan Har mountains area: an example from the Aba–Zoige Basin, Sichuan. Sedimentary Facies and Paleogeography 18, 1–18 (in Chinese with English abstract).

Enkelmann, E., Weislogel, A., Ratschbacher, L., Eide, E., Renno, A., Wooden, J., 2007. How was the Triassic Songpan-Ganzi basin filled? A provenance study. Tectonics 26 (TC4007). doi:10.1029/2006TC002078.

Floyd, P.A., Leveridge, B.E., 1987. Tectonic environment of the Devonian Gramscatho basin south Cornwall: framework mode and geochemical evidence from turbiditic sandstones. Journal of the Geological Society. London 144, 531–542.

Fedo, C.M., Eriksson, K.A., Krogstad, E.J., 1996. Geochemistry of shales from the Archean (~3.0Ga) Buhwa Greenstone Belt, Zimbabwe: implications of provenance and source-area weathering. Geochimica et Cosmochimica Acta 60, 1751–1763.

Fedo, C.M., Nesbitt, H.W., Young, G.M., 1995. Unravelling the effects of potassium metasomatism in sedimentary rocks and paleosols, with implications for paleoweathering conditions and provenance. Geology 23, 921–924.

Fedo, C.M., Young, G.M., Nesbitt, H.W., Hanchar, J.M., 1997. Potassic and sodic metasomatism in the Southern Province of the Canadian Shield: evidence from the Paleoproterozoic Serpent Formation, Huronian Supergroup, Canada. Precambrian Research 84, 17–36.

Gromet, L.P., Dymek, R.F., Haskin, L.A., Korotev, R.V., 1984. The North American shale composite: its composition, major and trace element characteristics. Geochimica et Cosmochimica Acta 48, 2469–2482.

Gu, X.X., 1994. Geochemical characteristics of the Triassic Tethys-turbidites in northwestern Sichuan, China; implications for provenance and interpretation of the tectonic setting. Geochimica et Cosmochimica Acta 58, 4615–4631.

Gu, X.X., Liu, J.M., Zheng, M.H., Tang, J.X., Qi, L., 2002. Provenance and tectonic setting of the Proterozoic turbidites in Hunan South China: geochemical evidence. Journal of Sedimentary Research 72, 393–407.

Hayashi, K., Fujisawa, H., Holland, H.D., Ohmoto, H., 1997. Geochemistry of ~1.9 Ga sedimentary rocks from northeastern Labrador, Canada. Geochimica et Cosmochimica Acta 61, 4115–4137.

Herron, M.M., 1988. Geochemical classification of terrigenous sands and shales from core or log data. Journal of Sedimentary Petrology 58 (5), 820–829.

Huang, J., Chen, B., 1987. The Evolution of the Tethys in China and Adjacent Regions. Geological Publishing House, Beijing, p. 109 (in Chinese).

Klimetz, M.P., 1983. Speculations on the Mesozoic plate tectonic evolution of eastern China. Tectonics 2 (2), 139–166.

Lan, Z.W., Chen, Y.L., Su, B.X., et al., 2006. The origin of sandstones from the Songpan-Ganze Basin, Sichuan, China: evidence from SHRIMP U-Pb dating of clastic zircons. Acta Sedimentology Sinica 24 (3), 321–332 (in Chinese with English abstract).

Liu, F., Chen, Y.L., Su, B.X., et al., 2006. Geochemistry and zircon ages of Triassic detrital sedimentary rocks from the Ganze-Songpan Block. Acta Geoscientica Sinica 27 (4), 289–296 (in Chinese with English abstract).

Lu, F.X., Sang, L.K., 2002. Petrology. Geological Publishing House, Beijing, 309–322 (in Chinese).

Ma, C.Q., Li, Z.C., Ehlers, C., Yang, K.G., Wang, R.J., 1998. A post-collisional magmatic plumbing system: Mesozoic granitoid plutons from the Dabieshan high-pressure and ultrahigh-pressure metamorphic zone, east-central China. Lithos 45, 431–456.

Ma, C.Q., Ehlers, C., Xu, C.H., Li, Z.C., Yang, K.G., 2000. The roots of the Dabieshan ultrahigh-pressure metamorphic terrane: constraints from geochemistry and Nd-Sr isotope systematics. Precambrian Research 102, 279–301.

Maynard, J.B., Valloni, R., Yu, H.S., 1982. Composition of modern deep-sea sands from arc-related basins. In: Leggett, J.K. (Ed.), Trench and forearc Geology: Sedimentation and Tectonics on Modern and Ancient Active Plate Margins, vol. 10. Geological Society of London, Special. Publications, pp. 551–561.

McElhinny, M.W., Embleton, B.J.J., Ma, X.H., Zhang, Z.K., 1981. Fragmentation of Asia in the Permian. Nature 293, 212–216.

McLennan, S.M., Hemming, S.R., McDaniel, D.K., Hanson, G.N., 1993. In: Geochemical approaches to sedimentation, provenance, and tectonics, vol. 284. Geological Society of America, Special Paper, pp. 21–40.

Meng, Q., Zhang, G., 2000. Geologic framework and tectonic evolution of the Qinling orogen, central China. Tectonophysics 323 (3–4), 183–196.

Nesbitt, H.W., Young, G.M., 1982. Early Proterozoic climates and plate motions inferred from major element chemistry of lutites. Nature 299, 715–717.

Nesbitt, H.W., Young, G.M., 1984. Prediction of some weathering trends of plutonic and volcanic rocks based on thermodynamic and kinetic considerations. Geochimica et Cosmochimica Acta 48, 1523–1534.

Nesbitt, H.W., Young, G.M., 1989. Formation and diagenesis of weathering profiles. The Journal of Geology 97, 129–147.

Nie, S.Y., Rowley, D.B., Yin, A., Jin, Y., 1993. History of northeastern Tibetan Plateau before India–Asia collision: formation of the Songpan-Ganzi flysch sequence and exhumation of the Dabie Shan ultra-high-pressure rocks. Geological Society of America Abstracts with Programs vol. 25, p. A117.

Nie, S., Yin, A., Rowley, D.B., Jin, Y., 1994. Exhumation of the Dabie Shan ultra-high-pressure rocks and accumulation of the Songpan-Ganzi flysch sequence, central China. Geology 22, 999–1002.

Roger, F., Jolivet, M., Malavieille, J., 2008. Tectonic evolution of the Triassic fold belts of Tibet. Comptes Rendus Geosciences 340 (2–3), 180–189.

Roger, F., Jolivet, M., Malavieille, J., 2010. The tectonic evolution of the Songpan-Garzê (North Tibet) and adjacent areas from Proterozoic to present: a synthesis. Journal of Asian Earth Sciences 39, 254–269.

Roser, B.P., Korsch, R.J., 1985. Plate tectonics and geochemical composition of sandstones: a discussion. The Journal of Geology. 93, 81–84.

Roser, B.P., Korsch, R.J., 1986. Determination of tectonic setting of sandstone-mudstone suites using SiO_2 content and K_2O/Na_2O ratio. The Journal of Geology 94, 635–650.

Roser, B.P., Korsch, R.J., 1988. Provenance signature of sandstone-mudstone suites determined using discriminant function analysis of major element data. Chemical Geology 67, 119–139.

Şengör, A.M.C., 1984. The Cimmeride Orogenic System and the Tectonics of Eurasia, vol. 195. Geological Society of America Special Paper.

She, Z.B., Ma, C.Q., Mason, R., et al., 2006. Provenance of the Triassic Songpan-Ganzi flysch, west China. Chemical Geology 231, 159–175.

Sichuan Bureau of Geology and Mineral Resources, 1984. The Regional Geological Surveying Reports Combining Zoige, Hongyuan, Aba, Longriba Geological Maps (1:200000) (in Chinese).

SINOPEC Exploration Southern Company, 2008. The investigation and evaluation of strategic oil and gas resources in Songpan-Aba area. Internal Report, 20–22 (in Chinese).

Su, B.X., Chen, Y.L., Lan, Z.W., et al., 2005. Sedimentary and geochemical study on the Precambrian-Triassic series of Songpan-Ganze block. Acta Sedimentology Sinica 23 (3), 437–446 (in Chinese with English abstract).

Tang, Y., 2011. The research on the Triassic very low-grade metamorphism in Zoige-Hongyuan area. Ph.D. thesis, China University of Geosciences, Wuhan. 29–40 (in Chinese).

Tang, Y., Sang, L.K., Liu, R., Yu, J.Sh., Yuan, Y.M., 2007. Application of mineral paragenesis analysis to the research of very low-grade metamorphism: taking Hongcan Well 1 in Songpan-Aba area as an example. Geoscience 21 (3), 457–461 (in Chinese with English abstract).

Taylor, S.R., McLennan, S.M., 1985. The Continental Crust: Its Composition and Evolution. Blackwell, Oxford. 1–312.

Wang, W., 2007. The Provenance of the Middle-Late Triassic Sediments and the Evolution of the Trace Elements and U-Pb Dating of Zircon in Zoige Basin M.S. thesis, China University of Geosciences, Wuhan, 19–32 (in Chinese).

Watson, M.P., Hayward, A.B., Parkinson, D.N., Zhang, Z.M., 1987. Plate tectonic history, basin development and petroleum source rock deposition onshore China. Marine and Petroleum Geology 4, 205–225.

Weislogel, A.L., 2008. Tectonostratigraphic and geochronologic constraints on evolution of the northeast Paleotethys from the Songpan-Ganzi complex, central China. Tectonophysics 451, 331–345.

Weislogel, A.L., Graham, S.A., Chang, E.Z., et al., 2006. Detrital zircon provenance of the late Triassic Songpan-Ganzi complex: sedimentary record of collision of the north and South China blocks. Geology 34, 97–100.

Wronkiewicz, D.J., Condie, K.C., 1989. Geochemistry and provenance of sediments from the Pongola Supergroup, South Africa: evidence for a 3.0-Ga-old continental craton. Geochimica et Cosmochimica Acta 53, 1537–1549.

Yang, F.Q., Wang, H.M., Yang, H.S., Xie, S.C., 1996. Late Triassic Carnian continental rise environment analysis of the Zhuwo formation in the Tanggor area, Zoige, Sichuan. Acta Sedimentology Sinica 14, 56–63 (in Chinese with English abstract).

Yang, F.Q., Xiong, W., 2000. Late Triassic deep-water trace fossils and their sedimentary environment in Jinmuda, Rangtang County, Sichuan, China. Acta Sedimentology Sinica 18, 73–79 (in Chinese with English abstract).

Zhou, D., Graham, S.A., 1996. Songpan-Ganzi Triassic flysch complex of the West Qinling Shan as a remnant ocean basin. In: Yin, A., Harrison, M. (Eds.), The Tectonic Evolution of Asia. Cambridge University Press, Cambridge, pp. 281–299.